

Cardiac Malformations and Myocardial Abnormalities in *Podoplanin* Knockout Mouse Embryos: Correlation With Abnormal Epicardial Development

Edris A.F. Mahtab,¹ Maurits C.E.F. Wijffels,² Nynke M.S. Van Den Akker,¹ Nathan D. Hahurij,³ Heleen Lie-Venema,¹ Lambertus J. Wisse,¹ Marco C. DeRuiter,¹ Pavel Uhrin,⁴ Jan Zaujec,⁴ Bernd R. Binder,⁴ Martin J. Schalij,² Robert E. Poelmann,¹ and Adriana C. Gittenberger-De Groot^{1*}

Epicardium and epicardium-derived cells have been shown to be necessary for myocardial differentiation. To elucidate the function of *podoplanin* in epicardial development and myocardial differentiation, we analyzed *podoplanin* knockout mouse embryos between embryonic day (E) 9.5 and E15.5 using immunohistochemical differentiation markers, morphometry, and three-dimensional reconstructions. *Podoplanin* null mice have an increased embryonic lethality, possibly of cardiac origin. Our study reveals impairment in the development of the proepicardial organ, epicardial adhesion, and spreading and migration of the epicardium-derived cells. Mutant embryos show a hypoplastic and perforated compact and septal myocardium, hypoplastic atrioventricular cushions resulting in atrioventricular valve abnormalities, as well as coronary artery abnormalities. The epicardial pathology is correlated with reduced epithelial–mesenchymal transformation caused by up-regulation of E-cadherin, normally down-regulated by *podoplanin*. Our results demonstrate a role for *podoplanin* in normal cardiac development based on epicardial–myocardial interaction. Abnormal epicardial differentiation and reduced epithelial–mesenchymal transformation result in deficient epicardium-derived cells leading to myocardial pathology and cardiac anomalies. *Developmental Dynamics* 237:847–857, 2008. © 2008 Wiley-Liss, Inc.

Key words: atrioventricular defects; E-cadherin; epithelial–mesenchymal transformation; cardiac development; proepicardial organ; posterior heart field

Accepted 28 December 2007

INTRODUCTION

Recently we studied podoplanin expression as a novel marker of a subset of myocardial cells of the embryonic mouse heart. We showed that podoplanin is specifically expressed in the sinus venosus myocardium and the developing cardiac conduction system (Gittenberger-de Groot et al., 2007).

Podoplanin is a mucin-like transmembrane glycoprotein of 43 kDa that was first described as E11 antigen in osteoblasts (Wetterwald et al., 1996). It is expressed in epithelial and mesothelial cells such as intestinal epithelium, alveolar type I cells (Williams et al., 1996), podocytes, and mesothelium of the visceral peri-

toneum (Breiteneder-Geleff et al., 1997). It was also shown to be a potent marker for lymphatic endothelium (Schacht et al., 2003). In addition, podoplanin expression was found in the epithelial lining of the coelomic wall of the pericardio–peritoneal canal and later on in the cells lining the pleural and pericardial cavity (Gitten-

¹Department of Anatomy and Embryology, Leiden University Medical Center, The Netherlands

²Department of Cardiology, Leiden University Medical Center, The Netherlands

³Department of Pediatric Cardiology, Leiden University Medical Center, The Netherlands

⁴Department of Vascular Biology and Thrombosis Research, University of Vienna, Austria

*Correspondence to: Adriana C. Gittenberger-de Groot, Department of Anatomy and Embryology, Leiden University Medical Center, P.O. Box 9600, Postzone S-1-P, 2300 RC Leiden, The Netherlands. E-mail: acgitten@lumc.nl

DOI 10.1002/dvdy.21463

Published online 7 February 2008 in Wiley InterScience (www.interscience.wiley.com).

TABLE 1. Cardiac Malformations and Survival Rate of the *podoplanin* KO Embryos Between E9.5–15.5^a

	E9.5 (n = 3)	E10.5 (n = 4)	E11.5 (n = 5)	E12.5 (n = 5)	E14.5 (n = 4)	E15.5 (n = 4)
Total KO hearts	3	—	—	—	—	—
Hypoplastic PEO	3	—	—	—	—	—
Dissociated EP	—	0	5	5	2	2
Perforated Myo	—	0	5	5	2	2
Dextroposed Ao	—	—	4	4	0	0
Hypoplastic AVC	—	—	4	4	0	0
Fenestrated VS	—	—	4	5	2	2
Hypoplastic CA media	—	—	—	—	3	4
Additional CA	—	—	—	—	2	2
KO embryos in litter	25%	24%	22.5%	18%	17%	16%

^aThe mutant hearts showed severe hypoplasia of the compact myocardium with several additional morphological abnormalities. The severe malformations at the early stages were correlated with the higher mortality of the mutant embryos at the earlier stages. KO, knockout; E, embryonic day; Ao, aorta; AVC, atrioventricular cushion; CA, coronary artery; EP, epicardium; Myo, myocardium; n, number of studied KO embryos; PEO, proepicardial organ; VS, ventricular septum. (—), not observed.

berger-de Groot et al., 2007). In a previous study, we showed that there is a close relationship between the podoplanin-positive cells lining the coelomic cavity epithelium and the podoplanin-positive and *Nkx2.5*-negative area that is added to the venous pole of the heart from the posterior heart field (PHF; Gittenberger-de Groot et al., 2007). This PHF is part of a more extensive area of the splanchnic mesoderm called the second heart field (Cai et al., 2003) or second lineage (Kelly, 2005; Cai et al., 2003).

It has been shown that the splanchnic mesoderm or mesenchyme of the dorsal mesocardium at the venous pole not only supports recruitment of sinus venosus myocardium but also the formation of the epicardium from the proepicardial organ (PEO) in chicken (Viragh and Challice, 1981; Kruithof et al., 2006) and mouse (Komiyama et al., 1987; Männer et al., 2001) embryos. Cells derived from the PEO grow out over the myocardial heart tube (Komiyama et al., 1987; Viragh et al., 1993; Vrancken Peeters et al., 1995; Kruithof et al., 2006) and have been shown to be essential for myocardial differentiation (Gittenberger-de Groot et al., 1998, 2000; Perez-Pomares et al., 2002; Lie-Venema et al., 2003; Eralp et al., 2005, 2006; Winter and Gittenberger-de Groot, 2007; Van Loo et al., 2007) after epithelial–mesenchymal transformation (EMT).

It is important to realize that it has been postulated that the PHF and resulting myocardium are derived from the epithelial lining of the coelomic

cavity (splanchnic mesothelium) by EMT (Gittenberger-de Groot et al., 2007). This process allows epithelial cells to become mobile mesenchymal cells, which can move through the extracellular matrix (Hay, 2005). An important feature of EMT is that the epithelial adherens junctions need to be loosened. In these junctions, the presence of E-cadherin is seen as a calcium-dependent cell to cell adhesion protein. Loss of E-cadherin results in loss of epithelial features (Cano et al., 2000) and consecutive development into migratory mesenchymal cells, whereas an up-regulated state of E-cadherin indicates an abnormal EMT (Van Loo et al., 2007). It has been shown that there is a functional link between the cell adhesion molecule E-cadherin and podoplanin. E-cadherin is down-regulated by podoplanin in human oral and mouse skin carcinomas, resulting in up-regulation of EMT leading to invasive growth and metastasis of the carcinoma cells (Martin-Villar et al., 2005). Podoplanin can, therefore, be presented as an inhibitor of E-cadherin thus stimulating the EMT process. This function might also be effective in the coelomic mesoderm-derived epicardium growing over the heart.

In this study, we studied *podoplanin* knockout mouse embryos at several developmental stages to elucidate the function of podoplanin in cardiac development. Podoplanin is expressed in the epicardium, and it may play a stimulating role in the EMT process. Therefore, we hypothesized that

knockout of *podoplanin* could lead to abnormal development of epicardium and disturbance of EMT from the epicardium resulting in a diminished formation, migration, and contribution of epicardium-derived cells (EPDCs) to the developing heart. This process might result in several EPDC-related cardiac malformations and myocardial abnormalities.

RESULTS

General Characteristics of the *podoplanin* Knockout Embryos

This *podoplanin* knockout mouse model is characterized by an increased embryonic and fetal death of approximately 40% of the homozygote embryos between stages E10–E16, with highest death rate between E10 and E13 (Table 1). In addition, 50% of the neonatal homozygote mutant mice die within the first weeks of life. Heterozygous mice reached sexual maturity. The cause of embryonic, fetal, and neonatal death (cardiac or non-cardiac) is presently not known.

Podoplanin was specifically expressed in the mesenchyme and in the myocardium at the venous pole. Podoplanin staining was seen in the PEO and the epicardium (Gittenberger-de Groot et al., 2007; Lie-Venema et al., 2007), which are mesenchymal in origin. In the myocardium at the venous pole, podoplanin stained the major parts of the cardiac conduction system and sinus venosus (SV) myocardium

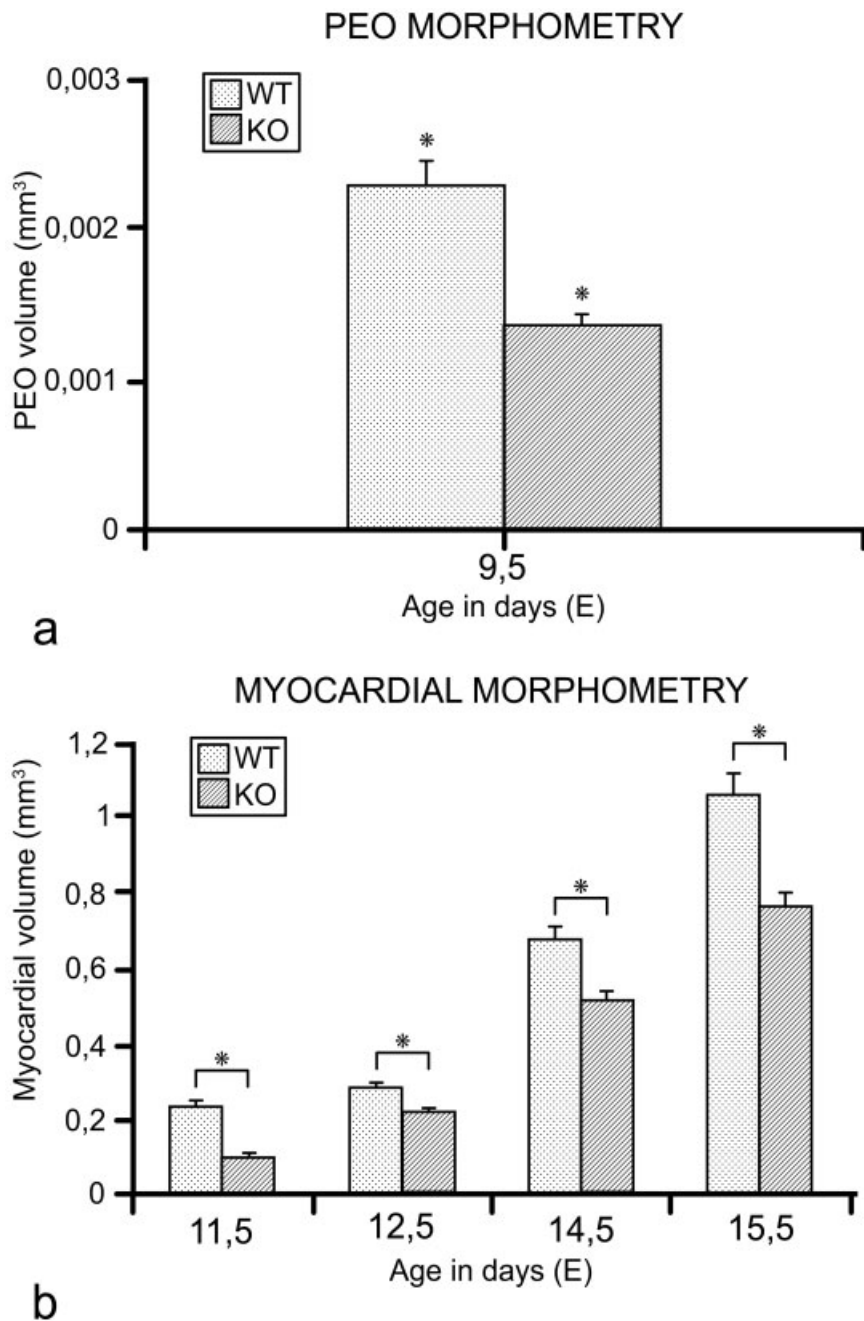


Fig. 1. A,B: Proepicardial organ (PEO, A) and myocardial (B) volume estimation of 15 wild-type (WT) mouse hearts of embryonic day (E) E9.5 (n = 3), E11.5 (n = 3), E12.5 (n = 3), E14.5 (n = 3), and E15.5 (n = 3), and 21 *podoplanin* knockout (KO) mouse hearts E9.5 (n = 3), E11.5 (n = 5), E12.5 (n = 5), E14.5 (n = 4), and E15.5 (n = 4). The *podoplanin* knockout embryos have a significantly (*) smaller PEO and myocardial volume ($P < 0.05$) compared with the WT embryos.

which includes the sinoatrial node (SAN), venous valves, myocardium in the dorsal mesocardium, the dorsal atrial wall, and primary atrial septum (AS) as well as the lining of the SV horns and the common pulmonary veins (PV).

We studied the embryonic phenotype of the knockout embryos with

regard to possible cardiac malformations in the *podoplanin* knockout embryos. Several marked morphological cardiac abnormalities were observed in the mutants. We encountered a significantly decreased PEO size and myocardial volume and thickness estimated by PEO and myocardial morphometry (Fig. 1a,b)

in the *podoplanin* null mice. Morphological study showed particularly in the younger stages a hypoplastic phenotype (thin atrial and ventricular myocardium) with epicardial impairments such as abnormal spreading and epicardial dissociation. These hearts also showed several morphological abnormalities such as severe dextroposition of the aorta, fenestration of the myocardium of the developing ventricular septum, and impaired formation and fusion of the atrioventricular cushions (Table 1). Moreover, myocardial hypoplasia and abnormalities were observed at the sinus venosus region, including the sinoatrial node, myocardium of the common pulmonary vein, the dorsal atrial wall, the primary atrial septum, and the myocardium of the sinus venosus horns. These malformations will be discussed in a separate study. Morphology and immunohistochemical expression patterns related to the contribution of PEO and epicardium to the heart are described below in the mutant mice and compared with the wild-type for subsequent stages of heart development.

Stage E9.5

Morphological abnormalities.

At E9.5, the PEO was clearly smaller in all *podoplanin* null mouse hearts (Fig. 2: 1 and 2), but no other morphological abnormalities were detected.

Immunohistochemistry.

At this stage, WT-1 was expressed in the PEO (Fig. 2a,b) of the wild-type mouse hearts and the *podoplanin* knockout mouse hearts (Fig. 2c,d). E-cadherin was clearly up-regulated in the PEO of the knockout mouse hearts compared with the wild-type (Fig. 2e–i,k). Podoplanin staining was observed in the PEO of the wild-type embryos (Fig. 2j). Other markers were unchanged in the knockout hearts compared with the wild-type (data not shown).

Stage E10.5

Morphological abnormalities.

At this stage, no morphological abnormalities were detected in the *podoplanin* null mouse embryos.

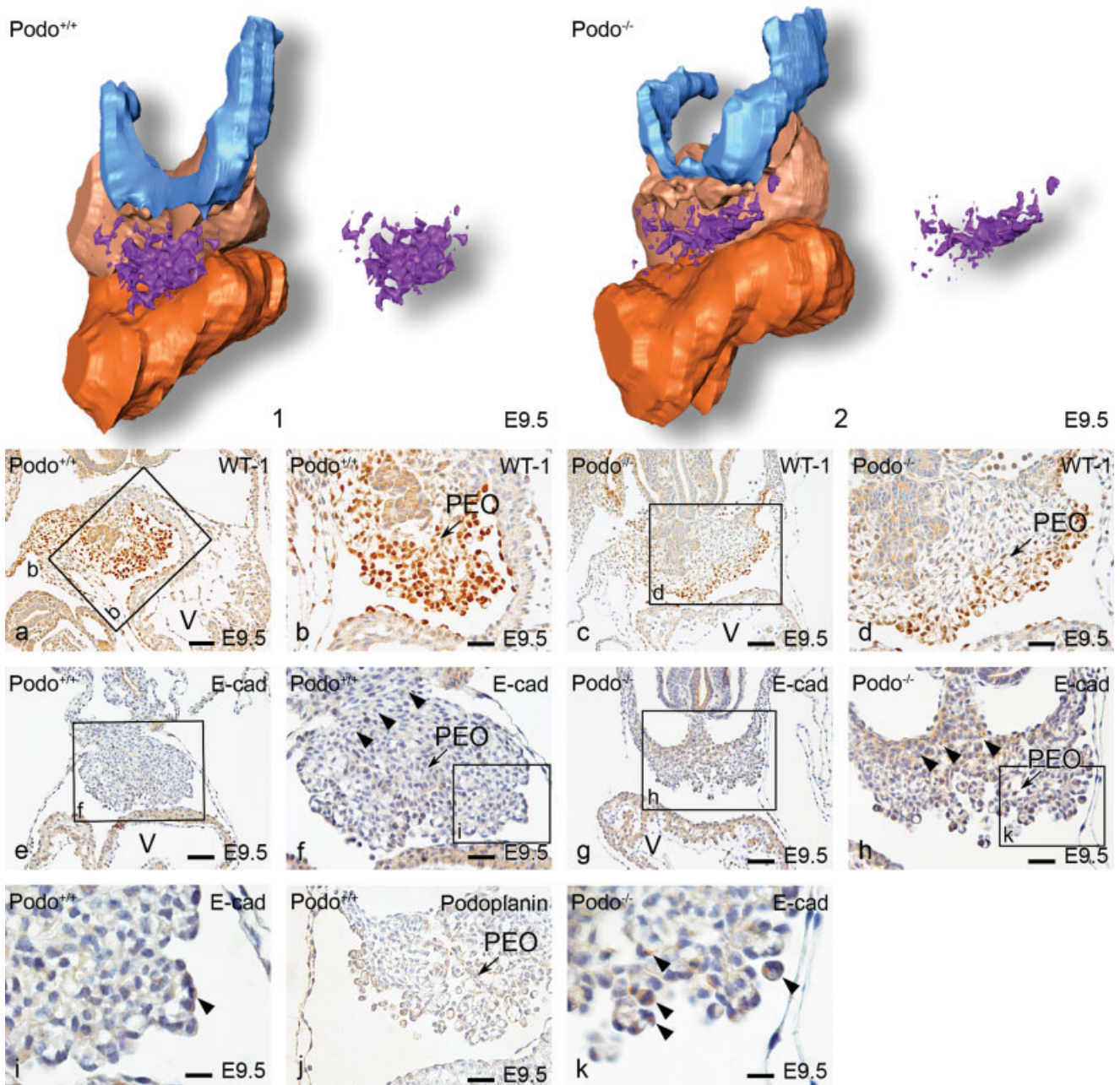


Fig. 2. a–k: Dorsal view of three-dimensional reconstruction (1,2) and ventral view of transverse sections of embryonic day (E) 9.5 *podoplanin* wild-type (WT, *Podo*^{+/+}) and knockout (KO, *Podo*^{-/-}) mouse hearts showing the expression of different markers and the size of the proepicardial organ (PEO). The smaller size of PEO in the KO heart (2) compared with the WT (1) is shown. Sections a,b: show WT-1 expression (a overview and b magnification) in the PEO of the WT mouse hearts. There are no marked differences in WT-1 expression between the WT and KO mouse hearts (c overview and d magnification). In contrast to WT-1, E-cadherin expression is up-regulated in the KO hearts (g,h,k) compared with the WT hearts (e,f,i). The E-cadherin up-regulation is also seen in the mesenchyme of the sinus venosus region (compare arrowheads in f with h) and in the PEO cells (compare arrowheads in i with k). In section j, podoplanin expression is shown in the PEO of the wild-type mouse heart. V, ventricle. Color codes: atrial myocardium, light brown; cardinal veins lumen/sinus venosus lumen, light blue; PEO, purple; and ventricular myocardium, dark brown. Scale bars = 200 μ m in a,c,e,g, 30 μ m in b,d,f,h,j, 10 μ m in i,k.

Immunohistochemistry.

As described earlier (Gittenberger-de Groot et al., 2007), at these stages weak podoplanin was observed in the major parts of the developing cardiac conduction system, and it was mark-

edly expressed in the epicardium (Fig. 3a and c, compare with WT-1 expression in Fig. 3b and d).

To demarcate the epicardium, coelomic epithelium and sites of active EMT, we additionally evaluated WT-1 staining as an epicardial and EPDC

marker and E-cadherin staining as a cell to cell adhesion marker playing a crucial role in EMT. In both wild-type and *podoplanin* knockout embryos, WT-1 was observed in the coelomic mesothelium and epicardium (Fig. 3b,d–f,i,j). However, due to the abnor-

mal covering of the epicardium, at several locations WT-1 expression followed this pattern and did thus not normally cover the myocardium in the knockout mouse embryos (Fig. 3d,e,i,j). Marked E-cadherin staining could be observed in both the epicardium and coelomic wall mesothelium of the *podoplanin* knockout embryos, whereas in wild-type mouse embryos these areas showed less E-cadherin (Fig. 3g,h,k,l).

Stage E11.5

Morphological abnormalities.

At this stage, the *podoplanin* knockout embryos showed an incomplete covering and dissociation of epicardium from the myocardium covering the atrial and ventricular walls. The compact atrial and ventricular myocardium and the trabeculae were hypoplastic. In addition, the atrioventricular endocardial cushions were widely separated and had not started to fuse, in contrast to wild-type hearts (data not shown).

Immunohistochemistry.

In both wild-type and knockout embryos, the immunohistochemical results of podoplanin (only for the wild-type), MLC-2a, Nkx2.5, WT-1, and E-cadherin were similar to the previous stages (data not shown).

Stage E12.5

Morphological abnormalities.

At this stage, the knockout embryos showed several morphological abnormalities (Fig. 4a,b). The aorta was more dextroposed in the knockout compared with the wild-type embryos and still positioned above the right ventricle (Fig. 4c,e). The aorta and pulmonary trunk showed in several cases a side by side position (data not shown). In the cases with severe hypoplasia of the atrial as well as ventricular compact myocardium and the trabeculae (Fig. 4c–f), epicardial dissociation and incomplete covering were markedly present (Fig. 4h–j). The myocardium of the atrial and ventricular wall showed several perforations that caused continuities between the subendocardial and the subepicardial layers (Fig. 4b and f compare with Fig. 4a and d). The developing ven-

tricular septum was fenestrated (Fig. 4b,e,m) compared with the wild-type (Fig. 4a,c,k). A common atrioventricular orifice was found in three of five cases, with marked atrioventricular cushion hypoplasia. Moreover, the MLC-2a-positive cells were absent in the atrioventricular cushion of the mutant heart (Fig. 4b and n, compare with Fig. 4a and l).

Immunohistochemistry.

In the wild-type embryos, podoplanin staining was marked in the epicardium covering the heart (Fig. 4g). Similar to the previous stages, we observed no differences in the immunohistochemical expression patterns of the used markers in the wild-type and knockout embryos.

Stage E13.5

Morphological abnormalities.

In the knockout embryos, there was partial epicardial dissociation without severe myocardial hypoplasia and morphological abnormalities (data not shown).

Immunohistochemistry.

The immunohistochemical expression of the used markers was similar in the wild-type and knockout embryos of E12.5 (data not shown).

Stage E14.5

Morphological abnormalities.

Partial epicardial dissociation was observed in two of the four studied hearts of knockout mice (Fig. 5a–f). These hearts also showed an abnormal atrial myocardial architecture; however, the hypoplasia was mild compared with stages E11.5 and E12.5 (Fig. 5a–d). The remaining two hearts showed normal epicardial morphology but still a decreased myocardial volume (Fig. 1b; Table 1). In addition, three knockout hearts showed a marked diminished presence of smooth muscle cells in coronary artery media, in two of these hearts additional (pin-point) coronary orifices were observed, and the third case showed a double left coronary orifice and an absent right coronary orifice (Table 1).

Immunohistochemistry.

In both the knockout and wild-type mice, the expression of MLC-2a and Nkx2.5 were similar to the previous stages. WT-1 was patchy in the mild hypoplastic hearts of the knockout embryos due to the partial epicardial discontinuity (Fig. 5e,f). Moreover, in the knockout hearts, less EPDCs were observed compared with wild-type (Fig. 5e,f).

E15.5

Morphological abnormalities.

At this stage, epicardial dissociation with mild hypoplasia of the compact myocardium was seen in two of four hearts studied. The remaining two hearts showed no epicardial morphological abnormalities but still had decreased myocardial volume (Fig. 1b). Similar to the previous stage, *podoplanin* knockout hearts showed coronary artery abnormalities (Table 1). All four studied hearts demonstrated deficiency of smooth muscle cells in the coronary artery media (Fig. 5g,h). Moreover, two hearts had additional (pin-point) coronary orifices.

Immunohistochemistry.

The expression patterns of the immunohistochemical markers in both wild-type and knockout embryos were similar to the previous stages, except that, in epicardial dissociation and incomplete covering of the mild hypoplastic hearts of the knockout embryos, WT-1 was not expressed (data not shown).

DISCUSSION

The coelomic epithelium not only forms the PEO (Viragh and Challice, 1981; Komiyama et al., 1987; Männer et al., 2001; Kruithof et al., 2006) but probably also contributes mesenchyme to the PHF-derived structures at the venous pole of the heart (Stalsberg and DeHaan, 1969; Cai et al., 2003; Kelly, 2005; Gittenberger-de Groot et al., 2007). The latter area is the source of sinus venosus myocardium, which is located at the venous pole. For that reason, we postulate that the PHF contributes to the formation of the PEO and sinus venosus myocardium. The PHF contribution to the sinus venosus myo-

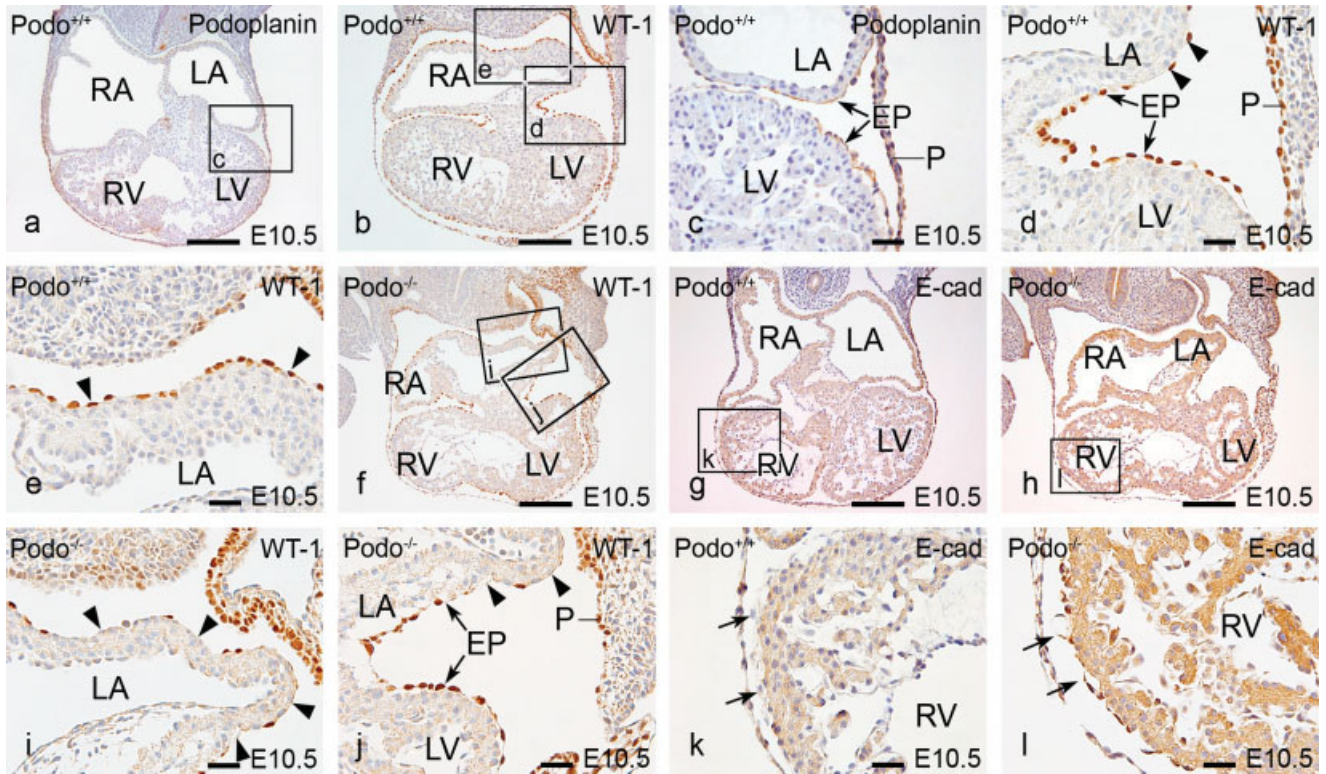


Fig. 3. a–l: Transverse sections of embryonic day (E) 10.5 wild-type (WT, a–e, g, k) and *podoplanin* knockout (f, h–j, l) mouse embryos. In WT mice, podoplanin and WT-1 are expressed in the epicardium (EP) and pericardium (P, a, b and arrows in magnification c, d). In the *podoplanin* knockout mouse, the WT-1 expression in the individual EP cells is unchanged (e, i and arrows in d, j). In the WT mouse, more EP cells are found (see arrowheads in d, e), as compared to bare areas in the knockout mouse (arrowheads in i, j). E-cadherin expression is more extensive in the EP of the *podoplanin* knockout embryos (h, overview; l, magnification, arrows) compared with the WT (g, overview; k, magnification, arrows). Moreover, epicardial dissociation due to the epicardial adhesion impairment can be recognized in the *podoplanin* knockout embryos (compare arrows in l with k). LA, left atrium; LV, left ventricle; RA, right atrium; RV, right ventricle. Scale bars = 200 μm in a, b, f–h, 30 μm in c–e, i–l.

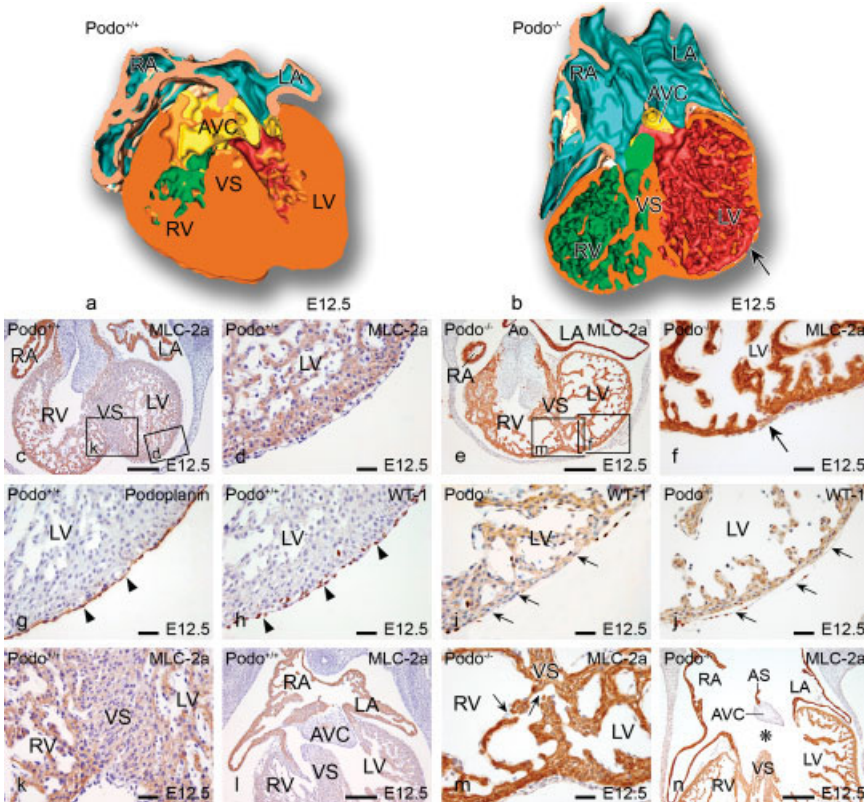


Fig. 4.

Fig. 4. a, b: Ventral view of a three-dimensional (3-D) reconstruction of an embryonic day (E) 12.5 wild-type (WT, a) and a *podoplanin* knockout (b) mouse heart. c–n: Transverse sections of the 3-D hearts stained with MLC-2a (except for g–j). Severe hypoplasia of the compact myocardium and the trabeculae (f, h–j) are present in the mutant mice. b, f: The chamber myocardium shows several perforations (arrows). The ventricular septum (VS) is markedly fenestrated (arrows in m magnification of e). Impaired fusion of atrial septum (AS), atrioventricular endocardial cushion (AVC) tissue, and VS results in a large common atrioventricular orifice (asterisk in n, compare a with b and l with n). Moreover, the MLC-2a-positive cells were absent in the AVC of the mutant heart (l, n). The aorta (Ao) is still positioned above the right ventricle (RV, e). Sections g and h show, respectively, podoplanin and WT-1 expression in the epicardium (arrowheads) of the WT mouse heart. In the knockout mouse (arrows in i and j), there is dissociation of the epicardium. LA, left atrium; LV, left ventricle; RA, right atrium. Color codes: atrial lumen, petrol; atrial myocardium, light brown; AV cushion, yellow; LV lumen, red; RV lumen, green; ventricular myocardium, dark brown. Scale bars = 200 μm in c, e, l, n, 30 μm in d, f, k, m.

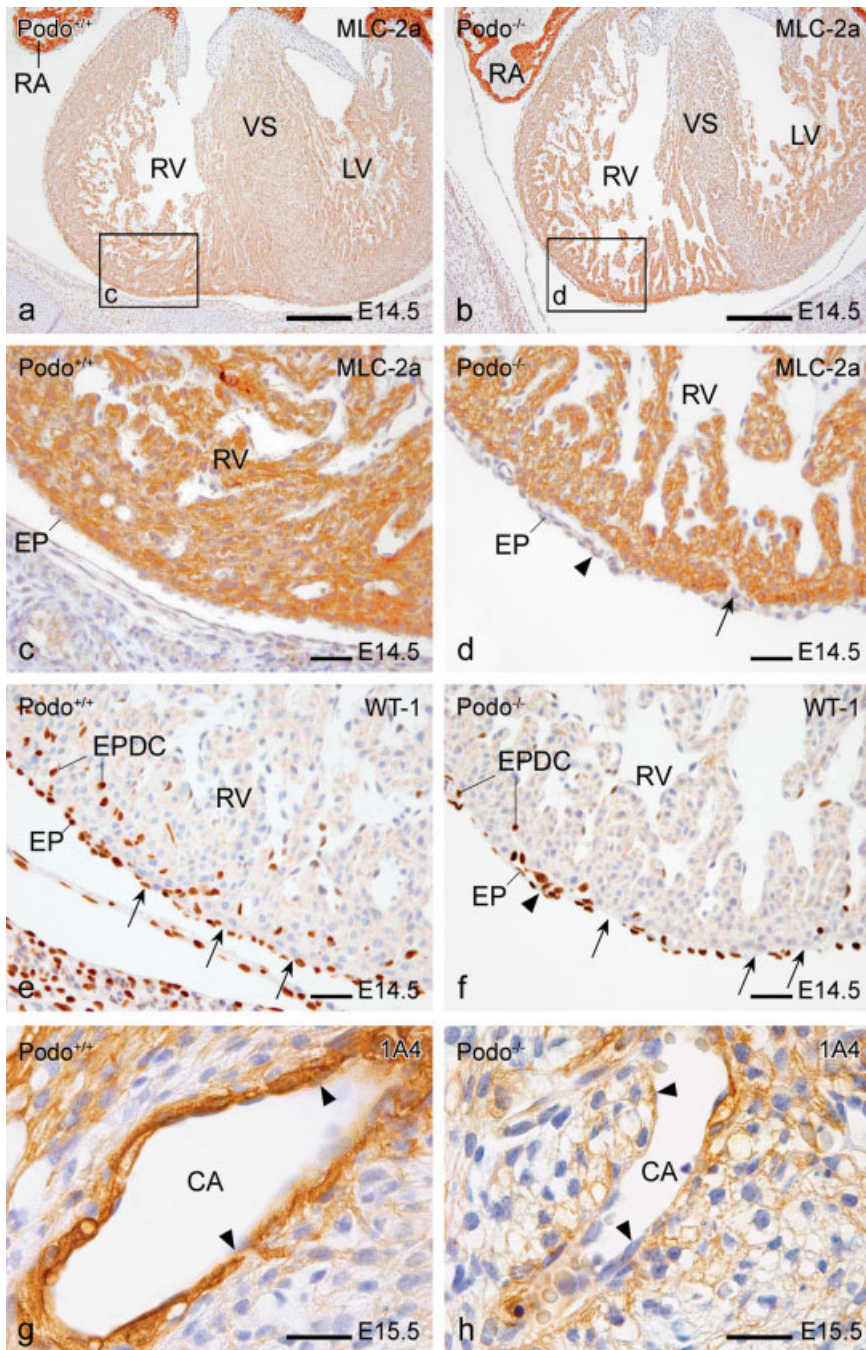


Fig. 5. Ventral view of transverse sections of an embryonic day (E) 14.5 wild-type (WT, **a,c,e**) and a *podoplanin* knockout (**b,d,f**) mouse heart stained with MLC-2a (**a-d**) and WT-1 (**e,f**). Hypoplasia of the compact myocardium and the trabeculae (compare **b** and **d** with **a** and **c**) as well as impaired epicardial spreading and dissociation shown in **d** and **f** are present in the mutant mouse. Moreover, the myocardium of the ventricular wall shows a perforation (arrow in **d**). The ventricular septum (VS) is less compact compared with WT (compare **a** and **b**). Sections **e** and **f** show WT-1 expression in the epicardium (EP) of the, respectively, WT and knockout mouse hearts. In the *podoplanin* knockout mouse (arrowhead in **d** and **f**), there is dissociation of the epicardium compared with the WT (**c** and **e**). In section **f**, there are several locations on the ventricular wall without epicardial covering (arrows in **f**) compared with WT (arrows in **e**). The *podoplanin* knockout hearts (**f**) have less epicardium-derived cells (EPDC) compared with WT (**e**). Transverse sections of an E15.5 WT (**g**) and knockout (**h**) embryos stained with 1A4 showing the deficiency of smooth muscle cells in the coronary artery (CA) media (arrowheads) in the knockout embryos. LV, left ventricle; RA, right atrium; RV, right ventricle. Scale bars = 200 μ m in **a,b**, 30 μ m in **c-f**, 10 μ m in **g,h**.

cardium at the venous pole, which has been shown to be derived from Nkx2.5-negative (Christoffels et al., 2006; Gittenberger-de Groot et al., 2007) and Tbx18-positive (Christoffels et al., 2006) progenitor cells, will be discussed in a separate study. In the current study, we have shown that the PEO as well as epicardium are positive for podoplanin, a marker of the coelomic mesothelium. Therefore, we investigated *podoplanin* knockout mice to study the effect of podoplanin on PEO, epicardium, EPDCs, and their described (Gittenberger-de Groot et al., 2000; Lie-Venema et al., 2003; Van Loo et al., 2007) subsequent influence on myocardial architecture.

PEO Migration, Epicardial Adhesion and Spreading Impairment

The PEO in mouse develops from the coelomic mesothelium at the venous pole of the heart (Komiya et al., 1987; Männer et al., 2001) in a bilaterally symmetric pattern (Schulte et al., 2007). After attachment to the myocardium, the PEO cells spread over the heart to cover the entire myocardium. The epicardial associated cardiac abnormalities reported in *podoplanin* knockout mouse are comparable to those in several other studies, where the importance of PEO cell migration and epicardial adhesion and spreading has been shown such as in VCAM-1, Tbx5, and α 4 integrin knockout mouse models (Kwee et al., 1995; Yang et al., 1995; Sengbusch et al., 2002; Dettman et al., 2003; Hatcher et al., 2004). Abnormal epicardial migration and spreading was recently described in the RXR α (Jenkins et al., 2005) and Fgf9 (Lavine et al., 2005) knockout mice that show malformations similar to those seen in our *podoplanin* knockout mouse supporting a role for *podoplanin* in the PEO migration, epicardial adhesion and spreading.

EPDCs Migration Impairment

The key process preceding the migration of EPDCs is EMT. Inhibition of EPDC migration has been shown as a result of a down-regulation of α 4 integrin leading to disturbed EMT (Dettman et al., 2003). Other important transcriptional factors involved in the

EMT are Slug (avian) and Snail (mammalian) that repress cell adhesion molecules including E-cadherin resulting in EMT (Batlle et al., 2000; Cano et al., 2000; Carmona et al., 2000). Of interest, in some tumors, repression of E-cadherin has been associated with up-regulation of *podoplanin* (Martin-Villar et al., 2005). In our study, we observed in the wild-type mouse the expected down-regulation of E-cadherin during the EMT period. In *podoplanin* knockout mouse, however, where fewer EPDCs were seen, E-cadherin expression remained high, supporting that podoplanin plays an important role in EMT.

Another transcription factor essential for the development of EPDCs is WT-1 (Moore et al., 1999), which is found in the epicardium and EPDCs shortly after EMT. Recently, we have shown a role for WT-1 in epicardial EMT and EPDC formation in the *SP3* mutant mouse (Van Loo et al., 2007). In that model, a down-regulation of WT-1 expression was observed resulting in disturbed epicardial–myocardial interaction, diminished EPDC formation and cardiac abnormalities comparable to our *podoplanin* knockout mouse. In the *podoplanin* model, we have not observed a down-regulation of WT-1 but lack of WT-1 expression in areas with absence of epicardium. Both models have in common a disrupted EMT and EPDC migration.

Cardiac Malformations

During heart development, cardiac looping has a crucial role, which is directed by several mechanisms such as gene regulation, myocardial contraction, and blood flow as recently reviewed by Linask and VanAuker (2007). Abnormal cardiac looping observed in this study could be the result of a myocardial problem related to a defective epicardial–myocardial interaction (Gittenberger-de Groot et al., 2000). It has been shown that EPDCs also invade the inner curvature (Lie-Venema et al., 2005). Remodeling of the inner curvature is an important process that is necessary to properly establish the definitive atrioventricular and ventriculo–arterial connections (Bartram et al., 2001; Van Loo et al., 2007). The outflow tract malformations as dextroposition of the aorta

and side by side position of the aorta and pulmonary trunk described in our study are thus considered to be the result of abnormal looping.

With regard to the coronary arteries in the *podoplanin* knockout embryos, we have observed severe abnormalities such as a hypoplastic media and additional (pin-point) orifices. Several retroviral labeling experiments, as well as studies in quail–chicken chimeras and PEO ablation studies have shown the contribution of EPDCs to the development of the smooth muscle cells and adventitial fibroblasts of the coronary arteries (Lie-Venema et al., 2007). Moreover, impaired formation of the coronary vasculature, as seen in the current study, was shown to be related to altered EPDC contribution and migration into the wall of the heart (Eralp et al., 2005; Lie-Venema et al., 2007).

Considering the atrioventricular cushions in the *podoplanin* mutant mice, we observed cases with an unseptated atrioventricular canal and a common atrioventricular valve. The relation to absence of EPDCs with valve defects observed in our study may, therefore, be twofold. First, the myocardium needs signals from the EPDCs for proper differentiation (Gittenberger-de Groot et al., 2000; Jenkins et al., 2005). EPDC deficiency in the underlying myocardium may influence the myocardial production of “adherons” and other chemotactic molecules such as transforming growth factor-beta and bone morphogenetic protein, which have been shown to be crucial for cushion development (Nakajima et al., 2000). Because our knockout model has a significantly diminished myocardial volume probably due to the epicardial dissociation and impaired EPDC formation, we can postulate that the hypoplasia of the atrioventricular cushion might be an indirect influence of EPDCs. Second, it has been shown that EPDCs invade the atrioventricular cushions directly where they may play a role in EMT of the endocardium (Gittenberger-de Groot et al., 1998; Männer et al., 2001; Perez-Pomares et al., 2002). Thus, based on our study, diminished direct physical presence of EPDCs in the cushions may also impair correct

cushion development, which may lead to hypoplasia of the cushions.

Additionally, the observed outflow tract and atrioventricular cushion abnormalities observed at the early stages of the mutant embryos could be the result of retarded development rather than malformations related to the EPDCs. However, the hearts at E11.5 and E12.5 showed the expected maturation: at E12.5, the atria and ventricles were present at the correct side and well distinguishable, the outflow tract cushions were well developed, the outflow tract was separated in aorta and pulmonary trunk, and the PV could be clearly observed at the left side. Considering these observation, we have concluded that the morphology of the mutant hearts was not based on just developmental delay. Combined with the fact that we did not see the severe malformations at the older stages, we conclude that increased embryonic death is related to the severe cardiac phenotype seen in part of the embryos at early stages.

We conclude that the observed cardiac abnormalities are the result of impairment in the PEO formation, migration, epicardial adhesion, and spreading and migration of EPDCs, finally resulting in increased embryonic death of the *podoplanin* knockout mouse embryos.

EXPERIMENTAL PROCEDURES

Generation of *podoplanin* Knockout (*podoplanin*^{-/-}) Mice

Overall, the size and exon–intron organization of the mouse *podoplanin* gene closely resembles that determined for the rat counterpart (Vanderbilt and Dobbs, 1998) and is given together with the strategy for gene disruption in Figure 6a.

The murine gene consists of six exons, separated by five relatively small introns (introns II to V) and a very long first intron I. Exon I encodes the predicted signal sequence, while the predicted extracellular domain is fully contained in exons II to IV. Exon V encodes the putative transmembrane domain and the almost complete cytoplasmic tail. The C-terminal last amino acid residue of mouse *podoplanin* including the

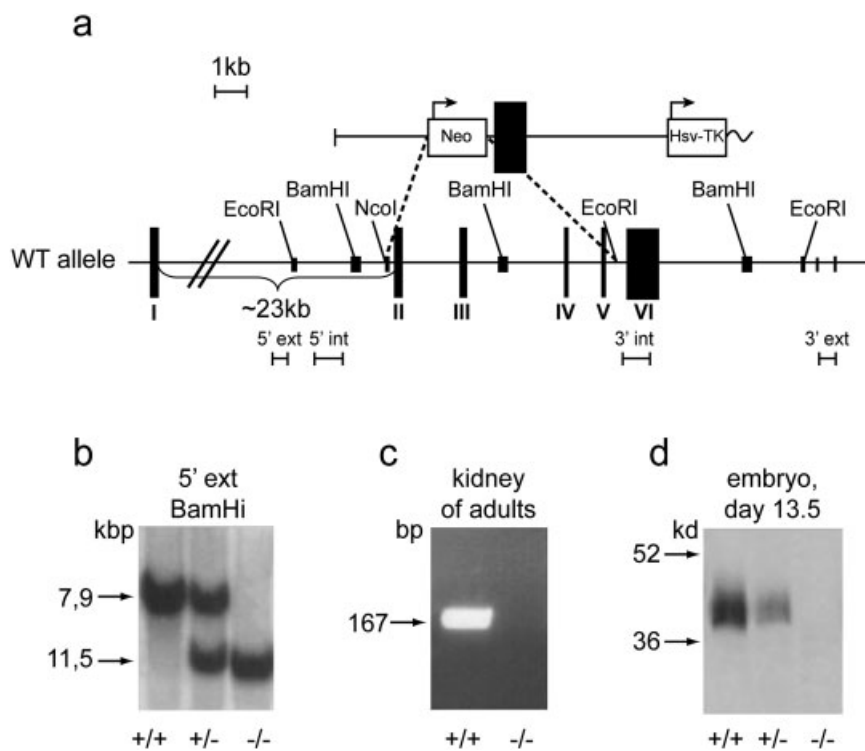


Fig. 6. Strategy of *podoplanin* gene disruption and gross appearance of *podoplanin*^{+/+} (*podo*^{+/+}) and *podoplanin*^{-/-} (*podo*^{-/-}) mice. **a:** Strategy of *podoplanin* gene disruption. Black boxes in the genomic structure represent exon sequences. Upon homologous recombination, the neo gene replaces a 7.7-kb genomic fragment encompassing exons II to V, leading to complete disruption of the *podoplanin* gene. **b:** Southern blot analysis of mouse genomic DNA digested with *Bam*HI and hybridized to a 5'-flanking external probe. **c:** Reverse transcriptase-polymerase chain reaction. **d:** Western blot on mouse tissues. In the adult kidney (shown as example), no *podoplanin* message is revealed in *podo*^{-/-} mice; in the Western blot experiments using whole embryos at embryonic day (E) 13.5 *podoplanin* protein is seen at the expected molecular weight in *podo*^{+/+} and *podo*^{+/-} mice, but is absent in *podo*^{-/-} mice. A clear gene dosing is seen in *podo*^{+/-} mice as compared to *podo*^{+/+} mice.

stop codon is encoded at the beginning of exon VI.

The *podoplanin* gene from 129S/v mouse genomic DNA was isolated and the pPNT.*podoplanin* targeting vector was constructed to inactivate the *podoplanin* gene in embryonic stem (ES) cells. It contains a 3.1-kb *Eco*RI-*Nco*I fragment containing the 3'-region of intron I, a neomycin phosphotransferase (neo) cassette, a 6.1-kb *Eco*RI fragment encompassing part of intron 5, the exon VI, and the 3'-untranslated region, and a herpes simplex virus thymidine kinase expression cassette (Fig. 6a). Two of 300 G418/Ganciclovir double-resistant clones underwent the desired homologous recombination, as confirmed by comprehensive Southern blotting of the isolated genomic DNA from R1 ES cells derived from the 129S/v mouse strain (received from A. Nagy, Samuel Lunenfeld

Institute, Toronto, Canada). Chimeric mice (F0), obtained by eight-cell stage embryo aggregation of the targeted ES cell clones, were test-bred for germline transmission with Swiss mice. They transmitted the disrupted *podoplanin* allele to their offspring (50% 129S/v: 50% Swiss genetic background), yielding *podoplanin*^{+/-} mice. Intercrossing of these mice resulted in *podoplanin*^{-/-} mice, as identified by Southern blot analysis of tail tip DNA using the 5'-external probe (Fig. 6b). Correct inactivation of *podoplanin* gene was further confirmed with additional digests using 5'-internal, neo-specific, 3'-internal and 3'-flanking external probes (not shown) and by reverse transcriptase-polymerase chain reaction (PCR; Fig. 6c) and Western blotting (Fig. 6d) using anti-*podoplanin* antibodies (Kerjaschki et al., 2004).

Genotyping of *podoplanin* knockout (*podoplanin*^{-/-}) Mice

Primers located in intron 2 of *podoplanin* gene detecting wild-type allele: 5'-GTT TAA AAG CCA GCA CTG GGC TGG G-3' and 5'-AAA ACA AGA AGG CAC GGA GAC TGC C-3' yield a 365-bp product present in *podoplanin*^{+/+} and *podoplanin*^{+/-} mice and neo-gene specific primers: 5'-CTA TTC GGC TAT GAC TGG GCA CAA C-3' and 5'-CTC AGA AGA ACT CGT CAA GAA GGC G-3' yield a 742-bp product present in *podoplanin*^{-/-} and *podoplanin*^{+/-} mice. PCR conditions to be used are initial 94 degrees for 2 min, then 35 cycles consisting of 94 degrees for 35 sec, 60 degrees for 35 sec, and 72 degrees for 35 sec.

General Description

We investigated the lining of the coelomic cavity and the morphology of the heart in 27 wild-type mouse embryos of embryonic stages E9.5 (n = 4), E10.5 (n = 4), E11.5 (n = 3), E12.5 (n = 4), E13.5 (n = 5), E14.5 (n = 4), and E15.5 (n = 3) and have compared these with 28 *podoplanin* knockout mouse embryos of stages E9.5 (n = 3), E10.5 (n = 4), E11.5 (n = 5), E12.5 (n = 5), E13.5 (n = 3), E14.5 (n = 4), and E15.5 (n = 4). All embryos were fixed in 4% paraformaldehyde and routinely processed for paraffin immunohistochemical investigation. In addition, 5- μ m transverse sections were mounted onto albumin/glycerin coated glass slides in a one to five order, so that five different stainings from subsequent sections could be compared.

Immunohistochemistry

After deparaffination and rehydration of the slides, microwave antigen retrieval was applied except for the anti-atrial myosin light chain 2 (MLC-2a) and *podoplanin* stainings, by heating them 12 min at 98°C in a citric acid buffer (0.01 M in aqua-dest, pH 6.0). Inhibition of endogenous peroxidase was performed with a solution of 0.3% H₂O₂ in phosphate buffered saline (PBS) for 20 min. The slides were incubated overnight with the following primary antibodies: 1/6,000 anti-MLC-2a as a myocardial marker

(which was kindly provided by S.W. Kubalak, Charleston, SC), 1/4,000 anti-human Nkx2.5 as our premyocardial marker (Santa Cruz Biotechnology, Inc., CA, SC-8697), 1/3,000 anti- α -smooth muscle actin (1A4, Sigma-Aldrich Chemie, USA, A 2547), 1/500 anti-podoplanin (clone 8.1.1. Hybridomabank, IA), 1/1,000 anti-Wilm's tumor suppressor protein as a marker for epicardium and early migrating EPDCs (WT-1, Santa Cruz Biotechnology, Inc., CA, SC-192), and 1/150 anti-E-cadherin as a cell adhesion marker (Santa Cruz Biotechnology, Inc., CA, SC-7870). All primary antibodies were dissolved in PBS-Tween-20 with 1% bovine serum albumin (BSA, Sigma Aldrich, St. Louis, MO). Between subsequent incubation steps all slides were rinsed in PBS (2 \times) and PBS-Tween-20 (1 \times). The slides were incubated with the secondary antibodies for 40 min: for MLC-2a, WT-1, and E-cadherin with 1/200 goat anti-rabbit biotin (Vector Laboratories, Burlingame, CA, BA-1000) and 1/66 goat serum (Vector Laboratories, S1000) in PBS-Tween-20; for Nkx2.5 with 1/200 horse anti-goat biotin (Vector Laboratories, BA-9500), and 1/66 horse serum (Brunschwig Chemie, Switzerland, S-2000) in PBS-Tween-20; for podoplanin with 1/200 goat anti-Syrian hamster-biotin (Jackson ImmunoResearch, West Grove, PA, 107-065-142), and 1/66 goat serum (Vector Laboratories, S1000) in PBS-Tween-20; for 1A4 1/250 rabbit anti-mouse PO (DAKO, P 0260) in PBS-Tween-20 with 1% BSA (Sigma Aldrich). Subsequently, except for 1A4 stained slides, all slides were incubated with ABC-reagent (Vector Laboratories, PK 6100) for 40 min. For visualization, the slides were incubated with 400 μ g/ml 3-3'-di-aminobenzidine tetrahydrochloride (DAB, Sigma-Aldrich Chemie, USA, D5637) dissolved in Tris-maleate buffer pH 7.6 to which 20 μ l of H₂O₂ was added: MLC-2a, WT-1, and E-cadherin 5 min; Nkx2.5, 1A4, and podoplanin 10 min. Counterstaining was performed with 0.1% haematoxylin (Merck, Darmstadt, Germany) for 5 sec, followed by rinsing with tap water for 10 min. Finally, all slides were dehydrated and mounted with Entellan (Merck, Darmstadt, Germany).

Three-Dimensional Reconstructions

We made three-dimensional (3-D) reconstructions of the atrial and ventricular myocardium of MLC-2a-stained sections of E12.5 wild-type as well as knockout embryos in which the morphological differences were shown. For the morphology of the PEO, we have made a 3-D reconstruction based on WT-1 staining of E9.5 wild-type and *podoplanin* knockout embryos. The reconstructions were made as described earlier (Jongbloed et al., 2004) using the AMIRA software package (Template Graphics Software, San Diego, CA).

PEO and Myocardial Morphometry

PEO volume estimation was performed in three wild-type and three *podoplanin* knockout mouse hearts of E9.5. Myocardial volume estimation was performed in 12 wild-type mouse hearts of embryonic stages E11.5 (n = 3), E12.5 (n = 3), E14.5 (n = 3), and E15.5 (n = 3), and 18 *podoplanin* knockout mouse hearts of embryonic stages E11.5 (n = 5), E12.5 (n = 5), E14.5 (n = 4), and E15.5 (n = 4). The morphometry for PEO as well as for myocardium was based on Cavalieri's principle as described by Gundersen and colleagues (Gundersen and Jensen, 1987). Briefly, regularly spaced (100 mm²) points were randomly positioned on the MLC-2a stained myocardium and on the WT-1 stained PEO. The distance between the subsequent sections of the slides was 0.075 mm for myocardium and 0.025 mm for PEO. The volume measurement was done using the HB2 Olympus microscope with a \times 100 magnification objective for myocardium and \times 200 for PEO (Fig. 1a,b). Statistical analysis was performed with independent sample *t*-test ($P < 0.05$) using the SPSS 11.0 software program (SPSS Inc, Chicago, IL).

ACKNOWLEDGMENT

We thank Jan Lens for expert technical assistance with the figures. N.M.S.-vdA. was funded by the Netherlands Heart Foundation (2001B057).

REFERENCES

- Bartram U, Molin DGM, Wisse LJ, Mohamad A, Sanford LP, Doetschman T, Speer CP, Poelmann RE, Gittenberger-de Groot AC. 2001. Double-outlet right ventricle and overriding tricuspid valve reflect disturbances of looping, myocardialization, endocardial cushion differentiation, and apoptosis in TGF β 2-knockout mice. *Circulation* 103:2745–2752.
- Batlle E, Sancho E, Franci C, Dominguez D, Monfar M, Baulida J, Garcia DH. 2000. The transcription factor snail is a repressor of E-cadherin gene expression in epithelial tumour cells. *Nat Cell Biol* 2:84–89.
- Breiteneder-Geleff S, Matsui K, Soleiman A, Meraner P, Poczewski H, Kalt R, Schaffner G, Kerjaszki D. 1997. Podoplanin, novel 43-kd membrane protein of glomerular epithelial cells, is down-regulated in puromycin nephrosis. *Am J Pathol* 151:1141–1152.
- Cai CL, Liang X, Shi Y, Chu PH, Pfaff SL, Chen J, Evans S. 2003. Isl1 identifies a cardiac progenitor population that proliferates prior to differentiation and contributes a majority of cells to the heart. *Dev Cell* 5:877–889.
- Cano A, Perez-Moreno MA, Rodrigo I, Locascio A, Blanco MJ, del Barrio MG, Portillo F, Nieto MA. 2000. The transcription factor snail controls epithelial-mesenchymal transitions by repressing E-cadherin expression. *Nat Cell Biol* 2: 76–83.
- Carmona R, Gonzalez-Iriarte M, Macias D, Perez-Pomares JM, Garcia-Garrido L, Munoz-Chapuli R. 2000. Immunolocalization of the transcription factor Slug in the developing avian heart. *Anat Embryol (Berl)* 201:103–109.
- Christoffels VM, Mommersteeg MT, Trowe MO, Prall OW, Gier-de Vries C, Soufan AT, Bussen M, Schuster-Gossler K, Harvey RP, Moorman AF, Kispert A. 2006. Formation of the venous pole of the heart from an Nkx2-5-negative precursor population requires Tbx18. *Circ Res* 98:1555–1563.
- Dettman RW, Pae SH, Morabito C, Bristow J. 2003. Inhibition of alpha4-integrin stimulates epicardial-mesenchymal transformation and alters migration and cell fate of epicardially derived mesenchyme. *Dev Biol* 257:315–328.
- Eralp I, Lie-Venema H, DeRuiter MC, Van Den Akker NM, Bogers AJ, Mentink MM, Poelmann RE, Gittenberger-de Groot AC. 2005. Coronary artery and orifice development is associated with proper timing of epicardial outgrowth and correlated Fas ligand associated apoptosis patterns. *Circ Res* 96:526–534.
- Eralp I, Lie-Venema H, Bax NA, Wijffels MC, van Der LA, DeRuiter MC, Bogers AJ, Van Den Akker NM, Gourdie RG, Schalij MJ, Poelmann RE, Gittenberger-de Groot AC. 2006. Epicardium-derived cells are important for correct development of the Purkinje fibers in the avian heart. *Anat Rec* 288A:1272–1280.

- Gittenberger-de Groot AC, Vrancken Peeters M-PFM, Mentink MMT, Gourdie RG, Poelmann RE. 1998. Epicardium-derived cells contribute a novel population to the myocardial wall and the atrioventricular cushions. *Circ Res* 82:1043–1052.
- Gittenberger-de Groot AC, Vrancken Peeters M-PFM, Bergwerff M, Mentink MMT, Poelmann RE. 2000. Epicardial outgrowth inhibition leads to compensatory mesothelial outflow tract collar and abnormal cardiac septation and coronary formation. *Circ Res* 87:969–971.
- Gittenberger-de Groot AC, Mathab EAF, Hahurij ND, Wisse LJ, DeRuiter MC, Wijffels MCEF, Poelmann RE. 2007. Nkx2.5 negative myocardium of the posterior heart field and its correlation with podoplanin expression in cells from the developing cardiac pacemaking and conduction system. *Anat Rec* 290:115–122.
- Gundersen HJ, Jensen EB. 1987. The efficiency of systematic sampling in stereology and its prediction. *J Microsc* 147:229–263.
- Hatcher CJ, Diman NY, Kim MS, Pennisi D, Song Y, Goldstein MM, Mikawa T, Basson CT. 2004. A role for Tbx5 in proepicardial cell migration during cardiogenesis. *Physiol Genomics* 18:129–140.
- Hay ED. 2005. The mesenchymal cell, its role in the embryo, and the remarkable signaling mechanisms that create it. *Dev Dyn* 233:706–720.
- Jenkins SJ, Hutson DR, Kubalak SW. 2005. Analysis of the proepicardium-epicardium transition during the malformation of the RXRalpha-/- epicardium. *Dev Dyn* 233:1091–1101.
- Jongbloed MRM, Schalijs MJ, Poelmann RE, Blom NA, Fekkes ML, Wang Z, Fishman GI, Gittenberger-de Groot AC. 2004. Embryonic conduction tissue: a spatial correlation with adult arrhythmogenic areas? Transgenic CCS/lacZ expression in the cardiac conduction system of murine embryos. *J Cardiovasc Electrophysiol* 15:349–355.
- Kelly RG. 2005. Molecular inroads into the anterior heart field. *Trends Cardiovasc Med* 15:51–56.
- Kerjaschki D, Regele HM, Moosberger I, Nagy-Bojarski K, Watschinger B, Soleiman A, Birner P, Krieger S, Hovorka A, Silberhumer G, Laakkonen P, Petrova T, Langer B, Raab I. 2004. Lymphatic neoangiogenesis in human kidney transplants is associated with immunologically active lymphocytic infiltrates. *J Am Soc Nephrol* 15:603–612.
- Komiyama M, Ito K, Shimada Y. 1987. Origin and development of the epicardium in the mouse embryo. *Anat Embryol (Berl)* 176:183–189.
- Kruithof BP, van Wijk B, Somi S, Kruithof-de Julio M, Perez Pomares JM, Weesie F, Wessels A, Moorman AF, van den Hoff MJ. 2006. BMP and FGF regulate the differentiation of multipotential pericardial mesoderm into the myocardial or epicardial lineage. *Dev Biol* 295:507–522.
- Kwee L, Baldwin HS, Min Shen H, Stewart CL, Buck C, Buck CA, Labow MA. 1995. Defective development of the embryonic and extraembryonic circulatory systems in vascular cell adhesion molecule (VCAM-1) deficient mice. *Development* 121:489–503.
- Lavine KJ, Yu K, White AC, Zhang X, Smith C, Partanen J, Ornitz DM. 2005. Endocardial and epicardial derived FGF signals regulate myocardial proliferation and differentiation in vivo. *Dev Cell* 8: 85–95.
- Lie-Venema H, Gittenberger-de Groot AC, van Empel LJP, Boot MJ, Kerkdijk H, de Kant E, DeRuiter MC. 2003. Ets-1 and Ets-2 transcription factors are essential for normal coronary and myocardial development in chicken embryos. *Circ Res* 92:749–756.
- Lie-Venema H, Eralp I, Maas S, Gittenberger-de Groot AC, Poelmann RE, DeRuiter MC. 2005. Myocardial heterogeneity in permissiveness for epicardium-derived cells and endothelial precursor cells along the developing heart tube at the onset of coronary vascularization. *Anat Rec* 282A:120–129.
- Lie-Venema H, van den Akker NMS, Bax NAM, Winter EM, Maas S, Kekarainen T, Hoeben RC, DeRuiter MC, Poelmann RE, Gittenberger-de Groot AC. 2007. Origin, fate, and function of epicardium-derived cells (EPDCs) in normal and abnormal cardiac development. *Scientific World Journal* 7:1777–1798.
- Linask KK, Vanauker M. 2007. A role for the cytoskeleton in heart looping. *ScientificWorldJournal* 7:280–298.
- Männer J, Perez-Pomares JM, Macias D, Munoz-Chapuli R. 2001. The origin, formation and developmental significance of the epicardium: a review. *Cells Tissues Organs* 169:89–103.
- Martin-Villar E, Scholl FG, Gamallo C, Yurrita MM, Munoz-Guerra M, Cruces J, Quintanilla M. 2005. Characterization of human PA2.26 antigen (T1alpha-2, podoplanin), a small membrane mucin induced in oral squamous cell carcinomas. *Int J Cancer* 113:899–910.
- Moore AW, McInnes L, Kreidberg J, Hastie ND, Schedl A. 1999. YAC complementation shows a requirement for Wt1 in the development of epicardium, adrenal gland and throughout nephrogenesis. *Development* 126:1845–1857.
- Nakajima Y, Yamagishi T, Hokari S, Nakamura H. 2000. Mechanisms involved in valvuloseptal endocardial cushion formation in early cardiogenesis: roles of transforming growth factor (TGF)-beta and bone morphogenetic protein (BMP). *Anat Rec* 258:119–127.
- Perez-Pomares JM, Phelps A, Sedmerova M, Carmona R, Gonzalez-Iriarte M, Munoz-Chapuli R, Wessels A. 2002. Experimental studies on the spatiotemporal expression of WT1 and RALDH2 in the embryonic avian heart: a model for the regulation of myocardial and valvuloseptal development by epicardially derived cells (EPDCs). *Dev Biol* 247:307–326.
- Schacht V, Ramirez MI, Hong YK, Hirakawa S, Feng D, Harvey N, Williams M, Dvorak AM, Dvorak HF, Oliver G, Detmar M. 2003. T1alpha/podoplanin deficiency disrupts normal lymphatic vasculature formation and causes lymphedema. *EMBO J* 22:3546–3556.
- Schulte I, Schlueter J, bu-Issa R, Brand T, Männer J. 2007. Morphological and molecular left-right asymmetries in the development of the proepicardium: a comparative analysis on mouse and chick embryos. *Dev Dyn* 236:684–695.
- Sengbusch JK, He W, Pinco KA, Yang JT. 2002. Dual functions of alpha4beta1 integrin in epicardial development: initial migration and long-term attachment. *J Cell Biol* 157:873–882.
- Stalsberg H, DeHaan RL. 1969. The pre-cardiac areas and formation of the tubular heart in the chick embryo. *Dev Biol* 19:128–159.
- Van Loo PF, Mahtab EA, Wisse LJ, Hou J, Grosveld F, Suske G, Philipsen S, Gittenberger-de Groot AC. 2007. Transcription factor Sp3 knockout mice display serious cardiac malformations. *Mol Cell Biol* 27:8571–8582.
- Vanderbilt JN, Dobbs LG. 1998. Characterization of the gene and promoter for RT140, a differentiation marker of type I alveolar epithelial cells. *Am J Respir Cell Mol Biol* 19:662–671.
- Viragh S, Challice CE. 1981. The origin of the epicardium and the embryonic myocardial circulation in the mouse. *Anat Rec* 201:157–168.
- Viragh S, Gittenberger-de Groot AC, Poelmann RE, Kalman F. 1993. Early development of quail heart epicardium and associated vascular and glandular structures. *Anat Embryol (Berl)* 188:381–393.
- Vrancken Peeters M-PFM, Mentink MMT, Poelmann RE, Gittenberger-de Groot AC. 1995. Cytokeratins as a marker for epicardial formation in the quail embryo. *Anat Embryol (Berl)* 191:503–508.
- Wetterwald A, Hoffstetter W, Cecchini MG, Lanske B, Wagner C, Fleisch H, Atkinson M. 1996. Characterization and cloning of the E11 antigen, a marker expressed by rat osteoblasts and osteocytes. *Bone* 18:125–132.
- Williams MC, Cao Y, Hinds A, Rishi AK, Wetterwald A. 1996. T1 alpha protein is developmentally regulated and expressed by alveolar type I cells, choroid plexus, and ciliary epithelia of adult rats. *Am J Respir Cell Mol Biol* 14:577–585.
- Winter EM, Gittenberger-de Groot AC. 2007. Cardiovascular development: towards biomedical applicability: epicardium-derived cells in cardiogenesis and cardiac regeneration. *Cell Mol Life Sci* 64:692–703.
- Yang JT, Rayburn H, Hynes RO. 1995. Cell adhesion events mediated by alpha4 integrins are essential in placental and cardiac development. *Development* 121:549–560.